High-Spin States in the Continuum. I. ^{20}Ne†

L. K. Fifield, R. W. Zurmühle, D. P. Balamuth, and J. W. Noé
Physics Department, University of Pennsylvania, Philadelphia, Pennsylvania 19174
(Received 31 August 1973)

We describe a new angular-correlation method for assigning spins to states that are selectively populated in reactions of the type $^{12}C(^{12}C,\alpha)\,^{20}Ne$ and which decay by the emission of an α particle to a state of nonzero spin, which decays in turn to a spin-zero state by the emission of a γ ray. Such states are not accessible to conventional particle-particle angular-correlation techniques. The new method consists of measuring the triple-angular correlation of the two α particles and the γ ray from the reaction $^{12}C(^{12}C,\alpha_1\alpha_2\gamma)\,^{16}O$ with the first emitted α particle observed at zero degrees, the γ ray observed at a fixed angle, and the second emitted α particle observed over a range of angles. Applications of this method to the determination of the spins of two states in ^{20}Ne, at 15.18 ± 0.02 MeV (6^+) and 17.40 ± 0.02 MeV (9^-), are discussed. The 17.40-MeV state has been identified as the 9^- member of the lowest negative-parity band in ^{20}Ne; the 6^+ assignment to the level at 15.18 MeV is in disagreement with an earlier assignment of spin and parity 9^- to this level.

[NUCLEAR REACTIONS $^{12}C(^{12}C,\alpha_1)\,^{20}Ne^*$ $(\alpha_2)\,^{16}O^*$ $(\gamma)\,^{16}O$ (g.s.), $E = 36.3$, 37.2 MeV; measured $\sigma(E_{\alpha_1}, E_{\alpha_2}, E_\gamma, \theta_{\alpha_1}, \theta_{\alpha_2}, \theta_\gamma, \varphi_\gamma)$. ^{20}Ne deduced levels J, π, branching ratios.]

I. INTRODUCTION

Following the observation[1] of rotational band structure in ^{20}Ne, considerable experimental effort has been directed towards locating the higher-spin members of known bands. In searching for high-spin levels at excitation energies where the density of low-spin states is large, it is desirable to have some means of preferentially populating states of high spin. Empirically, it has been observed that the $^{12}C(^{12}C,\alpha)^{20}Ne$ reaction is particularly suitable in this respect. Conventional angular-correlation techniques have been used to assign[2-5] spins to several states which were selectively populated in this reaction and which decay either by α-particle emission to the spin-zero ground state of ^{16}O, or by γ emission. The majority of these states were found to be high-spin states ($J \geq 4$). However, there are states which are selectively populated in the $^{12}C(^{12}C,\alpha)$ reaction which decay neither by γ emission nor by α emission to a spin-zero state, but instead decay by α emission to states with nonzero spin. The determination of the spins of such states has proved to be an experimental problem of some difficulty because the angular correlation of the two α particles, with the first emitted α particle detected at zero degrees, is not a sensitive function of the spin of the state in ^{20}Ne. In contrast, the same angular correlation for a state in ^{20}Ne with spin J which decays to the ^{16}O ground state is simply proportional to $[P_J(\cos\theta)]^2$ which is a very sensitive function of J. The physical situation for the two cases is depicted schematically in Fig. 1.

In this paper we describe a triple-correlation method which we have developed to assign spins to states which decay by α emission to states with nonzero spin, which decay in turn to a state with spin zero by emitting a γ ray. The method consists of measuring the angular distribution of the second emitted α particle (α_2) in coincidence with both the first emitted α particle (α_1) observed at zero degrees relative to the beam direction and the γ ray observed at a fixed angle. In a recent Letter,[6] we have reported spin assignments to two states in ^{20}Ne, at 15.18 and 17.40 MeV, that were obtained with this method. In this paper we discuss in considerably more detail than was possible in the context of a Letter, the theoretical form of the triple correlation, the experimental arrangement, and the acquisition and analysis of the data. In addition we present a more detailed account of the application of the method to the 15.18- and 17.40-MeV states in ^{20}Ne.

II. THEORY

We consider reactions of the type

$$^{12}C + {}^{12}C \rightarrow {}^{20}Ne^* + \alpha_1$$
$$\hookrightarrow {}^{16}O^*(3^-) + \alpha_2$$
$$\hookrightarrow {}^{16}O(\text{g.s.}) + \gamma$$

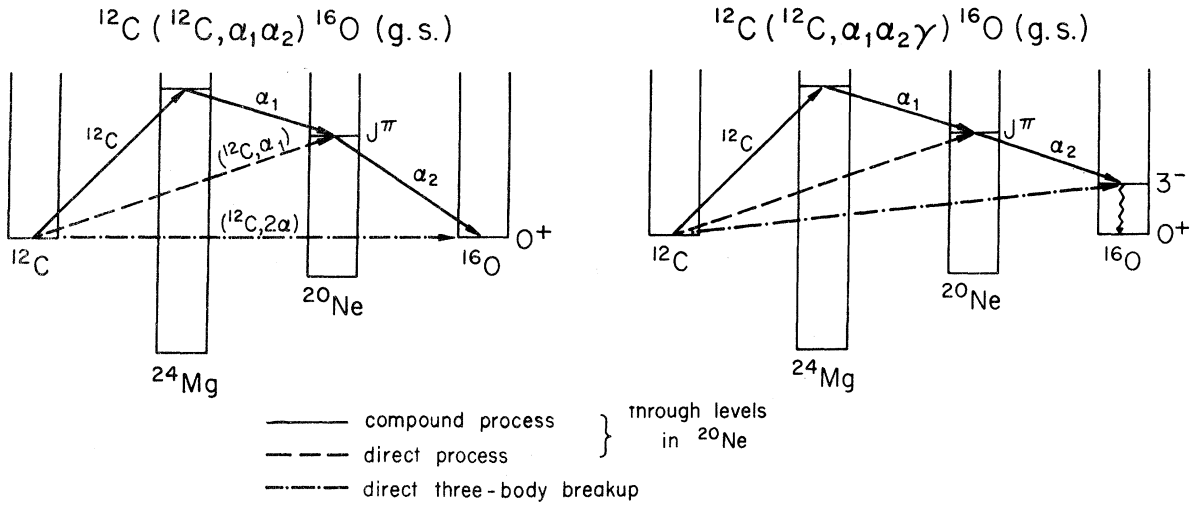

FIG. 1. Energy diagram illustrating the possible mechanisms by which the reactions $^{12}C(^{12}C,\alpha_1\alpha_2)^{16}O$ (g.s.) and $^{12}C(^{12}C,\alpha_1\alpha_2\gamma)^{16}O$(g.s.) may proceed.

and restrict ourselves to natural-parity states in the intermediate nucleus by requiring that α_1 be emitted at 0° relative to the beam direction. In this section, we compare the theoretical forms of the α_1-α_2 correlation (double correlation), and of the α_1-α_2-γ correlation (triple correlation), with α_1 observed at 0° in each case.

The theoretical form of the α_1-α_2 angular correlation, with the γ ray unobserved and α_1 observed at 0° in coincidence with α_2, is given by

$$W(\theta_{\alpha_1}=0^\circ,\theta_{\alpha_2},\varphi_{\alpha_2})=\sum_{\substack{LL'\\M}}(L-MJ_BM\,|\,J_A0)(L'-MJ_BM\,|\,J_A0)\langle\|L\|\rangle\langle\|L'\|\rangle^*$$
$$\times Y_L^{-M}(\theta_{\alpha_2},\varphi_{\alpha_2})Y_{L'}^{-M}{}^*(\theta_{\alpha_2},\varphi_{\alpha_2}), \tag{1}$$

where the spins of the state in ^{20}Ne and of the 3^- state in ^{16}O are denoted by J_A and J_B, respectively, and L, L' are the orbital angular momenta of α_2. The quantities $\langle\|L\|\rangle$ are the reduced matrix elements for the decay $^{20}Ne^*\rightarrow{}^{16}O^*+\alpha_2$ with α_2 carrying orbital angular momentum L. For $J_A\geq 3$, conservation of angular momentum and parity restrict the allowed values of L to J_A-3, J_A-1, J_A+1, and J_A+3, but the angular momentum barrier strongly favors the lowest allowed L value ($L_{\min}$). For the case in which only $L_{\min}$ contributes, Eq. (1) still contains an incoherent sum over the magnetic substates of the 3^- level in ^{16}O; the effect of this summation is to wash out the pronounced structure of the transitions to the individual substates. This is illustrated in Fig. 2(a), which shows the predicted double correlations for an 8^+ and a 9^- state in ^{20}Ne; it may be seen that the double correlation has no strong dependence on the spin of the state in ^{20}Ne.

The sum over the spin projections of the excited state in the final nucleus is incoherent because the γ ray is not observed. However, if the γ ray is also observed at a fixed angle, then the sum over the spin projections becomes a coherent sum. Provided the γ decay proceeds to a spin-zero state, the predicted α_1-α_2-γ angular correlation exhibits strong spin-dependent structure. This may be illustrated by consideration of the α_1-α_2-γ correlation when both α_1 and the γ ray are observed at 0°. Observation of the γ ray at 0° selects those α_2 decays which proceed to the $M=\pm1$ substates of the excited state in the final nucleus, from which it follows that the angular distribution of α_2's, in coincidence with both α_1 and the γ ray, must be proportional to $|Y^1_{L_{\min}}(\theta_{\alpha_2})|^2$ if the α decay proceeds by the lowest allowed L value only. More generally, the theoretical form for the α_1-α_2-γ angular correlation, with α_1 observed at 0° and the γ ray observed at a fixed angle, is given by

$$W(\theta_{\alpha_1}=0^\circ;\theta_{\alpha_2},\theta_\gamma,\varphi)=\sum_{LL'MM'kq}(L-MJ_BM|J_A0)(L'-M'J_BM'|J_A0)\langle\|L\|\rangle\langle\|L'\|\rangle^*(J_BMJ_B-M'|kq)(-1)^{J_B-M'}$$
$$\times\left(\frac{4\pi}{2k+1}\right)^{1/2}Y_L^{-M}(\theta_{\alpha_2},0)Y_{L'}^{-M'}{}^*(\theta_{\alpha_2},0)R_k(L_\gamma L_\gamma J_BJ_F)Q_kY_k^q(\theta_\gamma,\varphi), \tag{2}$$

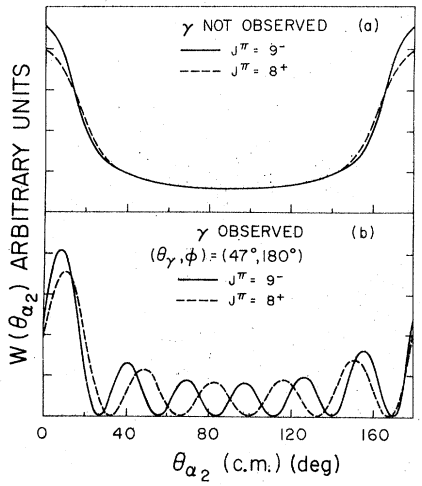

FIG. 2. (a) Theoretical α_1-α_2 correlations for the reaction $^{12}C(^{12}C,\alpha_1)\ ^{20}Ne^*\ [J^\pi]\ (\alpha_2)\ ^{16}O^*\ [3^-]$ with α_1 observed at zero degrees. (b) Theoretical α_1-α_2-γ correlations for the reaction $^{12}C(^{12}C,\alpha_1)\ ^{20}Ne^*\ [J^\pi]\ (\alpha_2)\ ^{16}O^*\ [3^-]\ (\gamma)\ ^{16}O$ [g.s.] with α_1 observed at zero degrees.

where φ is the relative azimuthal angle of the γ-ray detector and the α_2 detector. The spin of the final state [^{16}O(g.s.) in our example] is denoted by J_F, L_γ is the γ-ray multipolarity, and the attenuation factors Q_k take the finite solid angle of the γ-ray detector into account. The R_k are angular distribution coefficients as defined by Rose and Brink.[7] The remainder of the notation is the same as in Eq. (1). Equation (2) is derived in the Appendix.

The predicted triple correlations for an 8^+ and a 9^- state in ^{20}Ne decaying to the 3^- state in ^{16}O with the subsequent γ ray observed at $(\theta_\gamma, \varphi) = (133°, 0°)$ are shown in Fig. 2(b). It can be seen that the α_1-α_2-γ correlation is indeed a sensitive function of the spin of the state in the intermediate nucleus, provided that the γ decay proceeds to a spin-zero state. If this latter condition is not satisfied, then Eq. (2) contains an incoherent sum over the magnetic substates of the final state, which again washes out any pronounced spin-dependent structure. An example is provided by states in ^{24}Mg which α decay to the 4.25-MeV (4^+) state in ^{20}Ne.

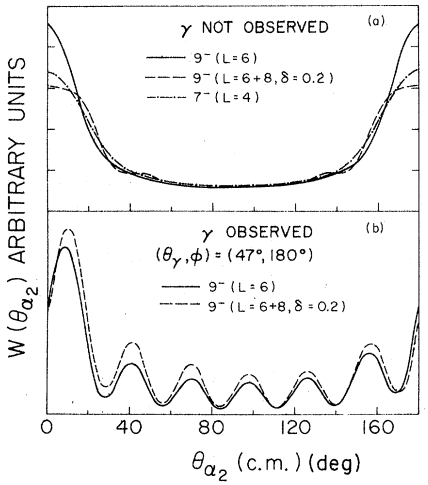

FIG. 3. Double $(\alpha_1$-$\alpha_2)$ and triple $(\alpha_1$-α_2-$\gamma)$ correlations showing the effect of L-value mixing in the decay $^{20}Ne^* \rightarrow {}^{16}O^*\ (3^-) + \alpha_2$. The effect of the finite size of the γ-ray detector has been included in the calculations of the triple correlations.

The triple correlation has a further desirable feature in that it is insensitive to small admixtures of the next higher allowed L value ($L_{min}+2$), a feature not possessed by the double correlation. Figure 3(a) compares the double correlations for a 9^- state decaying via L_{min} only, and via L_{min} plus an admixture of $L_{min}+2$ with a mixing ratio of 0.2. The same comparison is made in Fig. 3(b) for the triple correlation, which is clearly insensitive to the L-value admixture. The double correlation for a 7^- state decaying via the lowest allowed L value only is also shown in Fig. 3(a), and it is seen to be almost indistinguishable from the 9^- correlation with an admixture of $L_{min}+2$. This further illustrates the difficulties involved in attempts to assign spins from the α_1-α_2 double correlation.

III. EXPERIMENTAL PROCEDURE

A. Detector Geometry

A schematic of the experimental arrangement is shown in Fig. 4. A beam of ^{12}C ions from the University of Pennsylvania tandem accelerator was used to bombard a self-supporting carbon target about 40 μg/cm^2 thick. The first emitted α particle from the $^{12}C(^{12}C, \alpha_1\alpha_2\gamma)^{16}O$ reaction was detected at zero degrees relative to the beam

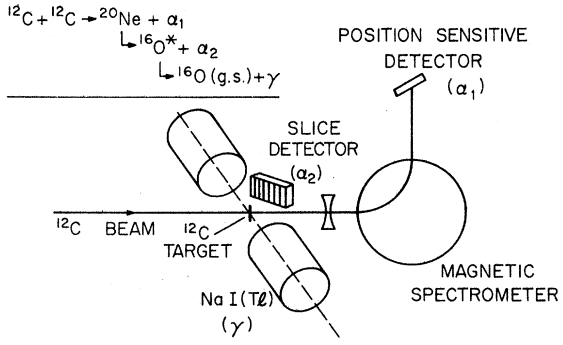

FIG. 4. The experimental arrangement used in the triple correlation measurements.

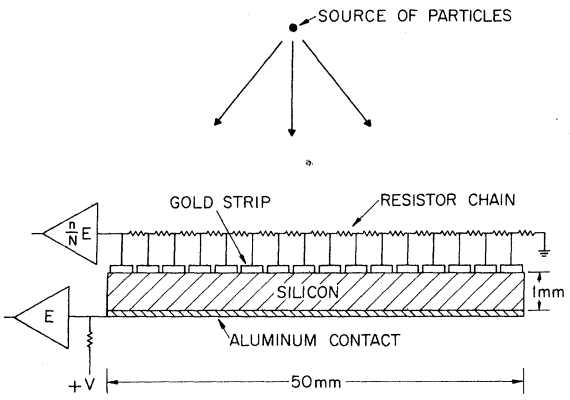

FIG. 5. Schematic diagram of the slice detector in cross section.

direction by a position-sensitive detector at the focus of a magnetic spectrometer. The γ rays were detected in two 7.6-cm×10.2-cm NaI(Tl) crystals placed at $(\theta_\gamma, \varphi) = (133°, 0°)$ and $(47°, 180°)$ at a distance of 11.4 cm from the target. These two angles are equivalent and the second detector served only to augment the count rate. The second emitted α particle (α_2) was detected in a "slice detector," a recently developed device capable of detecting particles at 16 angles simultaneously. This device is described in detail below. The center of the slice detector was 5 cm from the target at an angle of 50° to the beam direction, and the 16 angles spanned approximately 60° in the laboratory system. A strong magnetic field was maintained in front of the detector to protect it from electron bombardment, and a thin Ni foil was used to stop slow heavy ions. In addition, the detector was cooled to approximately −30° C with a thermoelectric element to suppress the

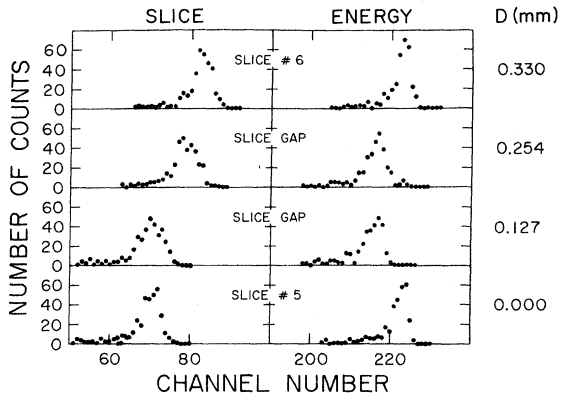

FIG. 6. Slice and energy spectra obtained as the gap between slices 5 and 6 of the slice detector was traversed with a highly collimated, monoenergetic α source. The quantity D is the distance (in mm) of the source from the starting position.

otherwise steadily increasing leakage current due to radiation damage.

B. Slice Detector

A slice detector is depicted schematically in Fig. 5. This device was constructed by evaporating the gold contact of the front electrode in 16 strips or "slices," each 3 mm wide and spanning the full width of the silicon wafer (approximately 1.6 cm), and separated by 0.025 cm. The slices were connected by a resistor chain, one end of which was grounded, while the other end was connected to a charge-sensitive preamplifier (P). A second preamplifier (E) was connected to the aluminum rear contact of the detector. The total charge deposited by a charged particle entering the n'th slice from the grounded end was collected by the E preamplifier, while only a fraction of the total charge was collected by the P preamplifier. The pulse height from the E preamplifier therefore corresponded to the particle energy, while the ratio of the two pulse heights identified the slice that recorded the event.

Compared to a continuous position-sensitive device this slice detector has the advantage that it assures reliable and reproducible definition of angle and solid angle even over long periods of time without the use of a multislit aperture that would considerably reduce the total solid angle. We were interested in the response of the slice detector to particles that impinge in the 0.025-

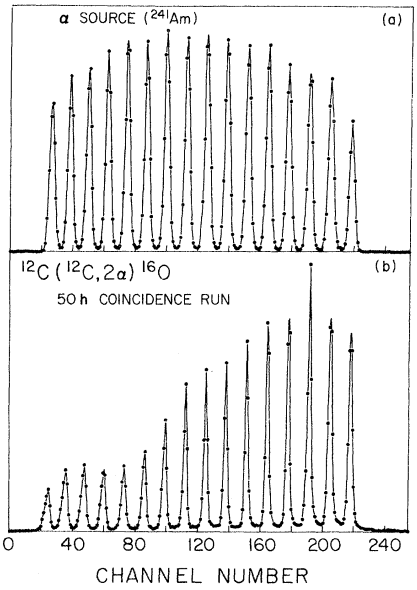

FIG. 7. (a) Undivided slice spectrum ($S \times E$) obtained with a monoenergetic α source. (b) Divided slice spectrum ($S \times E/E$) obtained in the course of the triple correlation measurement on the 17.40-MeV state in ^{20}Ne.

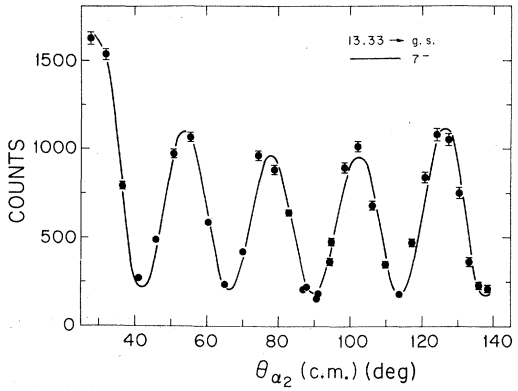

FIG. 8. Double $(\alpha_1-\alpha_2)$ correlation of the decays of the known 7^- state at 13.33 MeV in ^{20}Ne to the ^{16}O ground state. Two measurements were made, with the slice detector centered at $\theta_{lab}=45°$ and $\theta_{lab}=90°$. The solid curve is the best fit to $[P_7(\cos\theta)]^2$ + constant, integrated over the finite solid angle of a slice.

cm-wide gaps between adjacent gold contacts. One of these gaps was scanned with a ^{241}Am α source that was highly collimated with two sets of 0.005-cm-wide slits that were 2.5 cm apart. The results of this test are shown in Fig. 6. The detector is sensitive across the entire gap, contrary to conclusions of Hansen, Henderson, and Scott.[8] The charge collection is however slowed down which results in a reduction of the height of the energy pulse (E).

Typical slice spectra from the slice detector are shown in Fig. 7. Figure 7(a) is an undivided spectrum obtained with a monoenergetic ^{241}Am α-particle source, while Fig. 7(b) is the divided spectrum obtained from the 50-h triple correlation measurement on the 17.40-MeV state in ^{20}Ne. Each slice is seen to be completely resolved from adjacent slices. An accurate calibration of the solid angle of each individual slice was obtained using an α source mounted in the target position. To test the performance of the slice detector under experimental conditions, an α_1-α_2 angular-correlation measurement on the ground-state decays of the known[3] 7^- state at 13.33 MeV in ^{20}Ne was performed. This measurement is described in Sec. V, and the result is shown in Fig. 8. The solid line is a least-squares fit to a constant plus $[P_7(\cos\theta)]^2$ integrated over the finite solid angles of the slices.

C. Electronics and Data Acquisition

At the time these measurements were performed, only four analog-to-digital converters (ADC's) were available. The linear signals digitized for each event involving either an α_1-γ or an α_1-α_2 coincidence, or both, were the position×energy signal $(P_1\times E_1)$ from the detector at zero degrees, the mixed energy signal (E_γ) from the two NaI(Tl) crystals, and the energy (E_2) and slice×energy $(S\times E_2)$ signals from the slice detector. (For a 16 slice detector, $S=n/16$, where n labels the slices.) In addition, a routing module generated a digital word for each event which contained information on the type of coincidence. All four ADC's and the routing module were interfaced to a PDP-9 computer, which maintained a series of continuously incremented live displays which allowed the progress of the experiment to be monitored. All triple-coincidence events, and all double-coincidence events involving an α particle at zero degrees, were recorded on magnetic tape.

The coincidence conditions were imposed by four fast coincidence circuits; two flagged α_1-γ coincidences for the two NaI(Tl) crystals, a third flagged α_1-α_2 coincidences, and the fourth flagged triple coincidences. The logic diagram and the

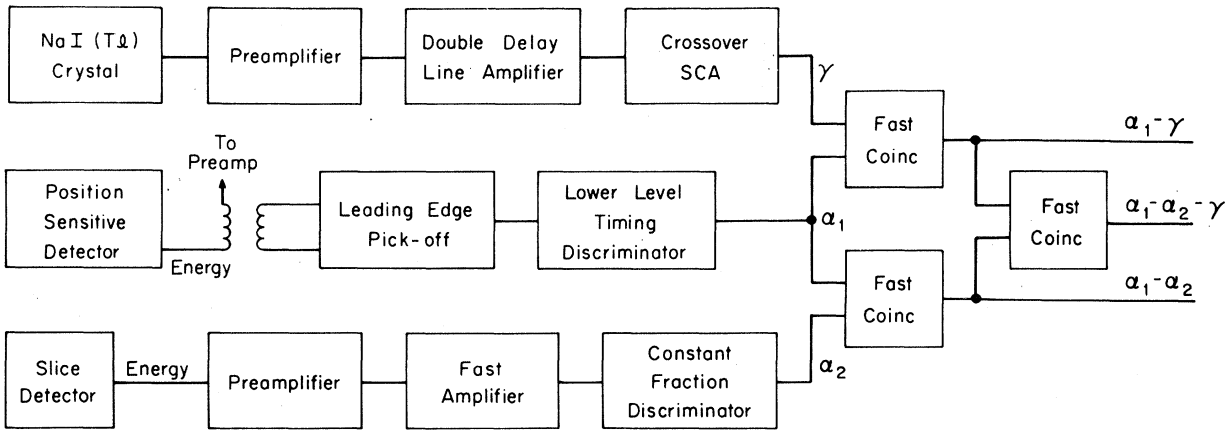

FIG. 9. Block diagram of the fast electronics employed to flag α_1-γ, α_1-α_2, or α_1-α_2-γ coincidences.

methods used to derive the timing signals from each of the detectors are shown in Fig. 9: For simplicity, only one NaI(Tl) crystal is shown. The timing methods used for the position-sensitive detector (PSD) at 0° and the slice detector merit some discussion.

Both detectors are large area (8.5 cm^2) devices, and each has a total capacitance of about 200 pF at a depletion depth of 550 μm. In both detectors, this capacitance forms a distributed RC circuit with the position-dependent, charge-dividing resistance. The risetime of the charge pulse (E) thus varied from a minimum, equal to the risetime of the electronics (50 nsec) for signals from the ends, to a maximum of about 300 nsec for signals from the center. Because of this variation in risetime, crossover timing was unsuitable for these detectors. Instead, the leading edge timing illustrated in Fig. 9 was employed for the PSD, and was found to be very satisfactory for the small dynamic range of energy pulses from this detector. In contrast, the energy pulses from the slice detector spanned a wide dynamic range and it was necessary to use constant fraction timing. The resolving times of the coincidence circuits used throughout the experiment were 75 nsec for α_1-γ coincidences and 60 nsec for α_1-α_2 coincidences. The trues-to-random ratios within these resolving times were found to be better than 10:1 for both α_1-γ and α_1-α_2 coincidences. The number of random triple coincidences expected with the above resolving times was estimated and found to be negligible.

D. Determination of the Effect of Hyperfine Interaction

The nuclear lifetime of the 6.13-MeV state in ^{16}O is rather long (25 ± 2 psec[9]), and consequently the possibility of attenuation of the triple correlation by hyperfine interaction (HFI) must be considered. At the beam energies used for the triple-correlation measurements on the 17.40- and 15.18-MeV states in ^{20}Ne, the average energy of the recoiling ^{16}O* (6.13-MeV) ions was about 6 MeV. At this energy, 52% of the ^{16}O* ions emerging from the target are predicted[10] to be in the 5^+ ionic-charge state, with most of the remainder divided equally between 4^+ and 6^+ charge states. The resulting electronic configurations would be expected[11] to generate magnetic fields at the nucleus which would be sufficient to produce significant attenuation of the triple correlation.

In order to obtain an estimate of the effect of HFI on the triple correlation, we measured the angular correlation of 6.13-MeV γ rays from the reaction ^{16}O(α, $\alpha'\gamma$)^{16}O, with the inelastically scattered α particles populating the 6.13-MeV level observed at 180° in an annular surface-barrier detector. The γ rays were detected in an array of four 7.6×10.2-cm NaI(Tl) crystals,[12] and measurements were made at two sets of angles. The beam energy of 14.0 MeV was chosen so that the energy of the recoiling ^{16}O* ions was approximately 6 MeV.

The theoretical angular correlation of the γ rays in coincidence with the α particles observed at 180° may be written

$$W(\theta) = \sum_{k=0}^{2J_B} (J_B 0\, J_B 0 \,|\, k0) Q_k R_k (L_\gamma L_\gamma J_B J_F) P_k(\cos\theta), \tag{3}$$

where the R_k are angular-correlation coefficients defined by Rose and Brink.[7] The effect of the hyperfine interaction may be included in both Eqs. (2) and (3) through the attenuation coefficients Q_k, which may be written

$$Q_k = Q_k(\text{finite geometry}) \times Q_k(\text{HFI}). \tag{4}$$

The Q_k(finite geometry) take the finite size of the NaI(Tl) crystal into account and may be readily calculated for a given geometry. In fitting Eq. (3), with the Q_k given by Eq. (4), to the experimental correlation, the only free parameters are a normalization and the Q_k(HFI) ($k = 2, 4, \ldots 2J_B$), and these are to be determined from the fit. The values for the Q_k(HFI) determined in this way were then used in fitting the triple correlations of decays to the 6.13-MeV (3^-) state in ^{16}O.

IV. DATA REDUCTION

The PDP-9 computer used in the acquisition of the data was also used in the off-line analysis. The data reduction consisted of obtaining angular distributions of the second emitted α particle (α_2) in coincidence with both a given group in the zero-degree ($P_1 \times E_1$) spectrum and a given range of E_γ. This was accomplished by setting digital windows on each of the 16 peaks in the divided slice spectrum ($S \times E_2/E_2$), thereby defining the individual slices. Sixteen E_2 spectra, one for each slice of the slice detector, were then played back from tape for double coincidence events which satisfied the condition on $P_1 \times E_1$. Simultaneously, a further 16 spectra were accumulated for triple-coincidence events which satisfied the conditions on both $P_1 \times E_1$ and E_γ.

Typical results are shown in Figs. 10 and 11. Figure 10 is an isometric display of the E_2 spectra of all 16 slices for double coincidences, while Fig. 11 shows E_2 spectra from a single slice for double and triple coincidences. The peaks in these spectra are due to particle decays from the se-

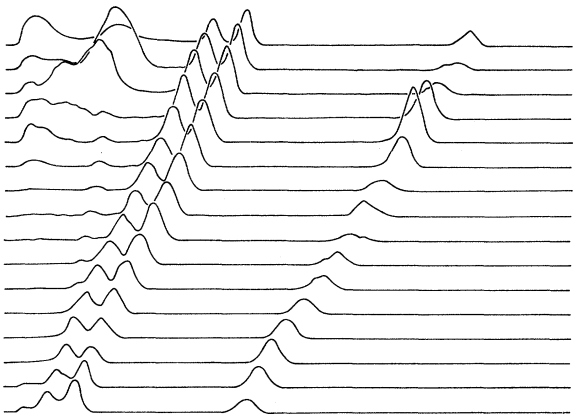

FIG. 10. Energy spectra for double coincidence events from each of the 16 slices of the slice detector, obtained in the course of the triple-correlation measurement on the 15.18-MeV state in ^{20}Ne. Decays to the ^{16}O ground state, 6.05–6.13-MeV doublet, and 6.92–7.12-MeV doublet, and decays to the ^{19}F ground state are all clearly visible.

lected region of excitation energy in the intermediate nucleus to known states in the final nucleus; α decays to states in ^{16}O and proton decays to states in ^{19}F are visible in both Figs. 10 and 11. As expected, there is no peak corresponding to decays to the ^{16}O ground state in the E_2 spectrum of triple coincidences.

The triple correlations were extracted from the E_2 spectra of triple coincidences by summing the peaks corresponding to a given decay mode in each of the 16 slices. After conversion from the laboratory to the center-of-mass system, the resulting triple correlations were fitted to the sum of an isotropic background and Eq. (2) integrated over the finite solid angle of a slice. It was assumed that the α_2 decays proceeded by the lowest allowed L value, but it was shown in Sec. II that small admixtures of the next higher allowed L value have a negligible effect on the predicted correlation. Large admixtures of the next higher allowed L value were considered extremely unlikely because of the considerably higher angular momentum barrier. The only parameters in the fit were then the spin of the state in the intermediate nucleus, the magnitude of the isotropic background term, and an over-all normalization.

The isotropic background term was included to take into account processes other than the decay of the state of interest in the intermediate nucleus. In particular, α particles in the selected region of the $P_1 \times E_1$ spectrum could arise from the formation of broad low-spin states in the intermediate nucleus, from direct three-body breakup of a ^{24}Mg compound nucleus, or from α_2 decays of a state in ^{20}Ne with α_2 emitted at zero degrees. All three processes could produce true triple coincidences, and there was no unambiguous prescription for subtracting their contribution to the triple correlation. Some justification for the assumption of an isotropic background to the triple correlation was, however, provided by the absence of strong angle-dependent structure in the triple correlations from flat regions of the zero degree

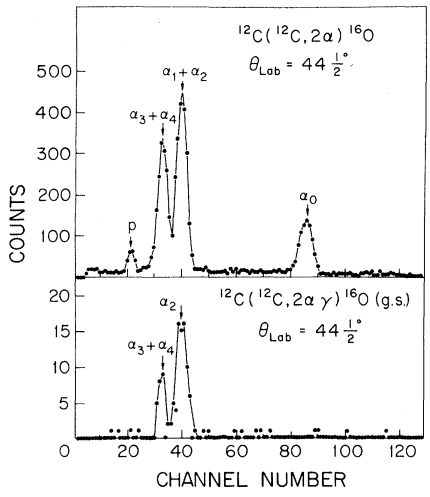

FIG. 11. (a) The energy spectrum of a single slice, taken from Fig. 10. (b) The corresponding energy spectrum of triple coincidence events. Any possible contribution of decays to the 6.05-MeV state in ^{16}O has been excluded by setting the γ-ray window above the 511-keV photopeak.

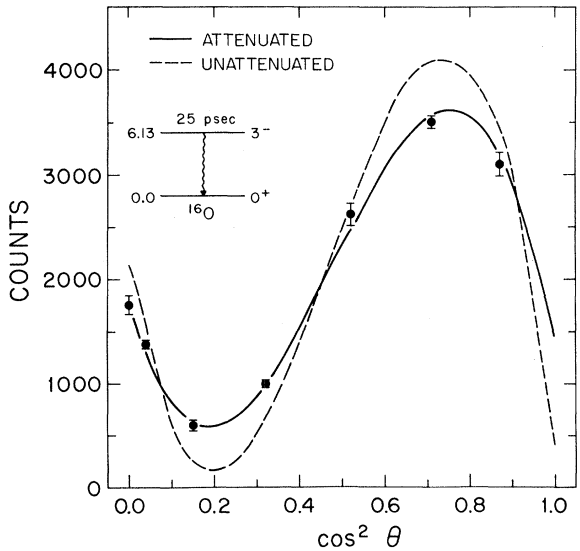

FIG. 12. Experimental and theoretical angular correlations of decays of the 6.13-MeV (3$^-$) state in ^{16}O, populated in the ^{16}O(α,α')^{16}O*(6.13-MeV) reaction with α' observed at 180°.

spectrum.

Information on the branching ratios of the various α decays from the state of interest in ^{20}Ne was extracted from the data. However, it was not sufficient simply to sum the total number of counts in the α_1-α_2 correlation for a given decay mode and correct for angular-correlation effects. Such a procedure would include contributions from processes, other than the formation of the particular state in ^{20}Ne, which also produced α particles in the selected region of the zero degree spectrum. These contributions could, however, be estimated from a zero degree spectrum in coincidence with the α_2's of a given decay mode. To obtain such a spectrum, it was necessary to set a further 16 windows on E_2, one for each slice, to follow the kinematic locus of the peaks corresponding to a given decay mode. The number of decays from the selected state in ^{20}Ne were then obtained by summing the peak in the resulting zero degree spectrum, and subtracting a background estimated from the flat regions on either side of the peak.

V. RESULTS

The preceding method has been applied to two states in ^{20}Ne, at 17.40 ± 0.02 and 15.18 ± 0.02 MeV. Prior to our measurements, a state at 15.18 MeV had been assigned $J^\pi = 9^-$ by Panagiotou, Gove, and Harar.[13]

A. Determination of the Q_k

The angular correlation of 6.13-MeV γ rays from the reaction ^{16}O$(\alpha, \alpha'\gamma)^{16}$O at a bombarding energy of 14 MeV is shown in Fig. 12. The solid curve is the best fit to Eq. (3) with the Q_k given by Eq. (4); the values of the Q_k(HFI) extracted from the fit are $Q_2(\text{HFI}) = 0.88 \pm 0.04$, $Q_4(\text{HFI}) = 0.74 \pm 0.24$, $Q_6(\text{HFI}) = 0.68 \pm 0.04$.

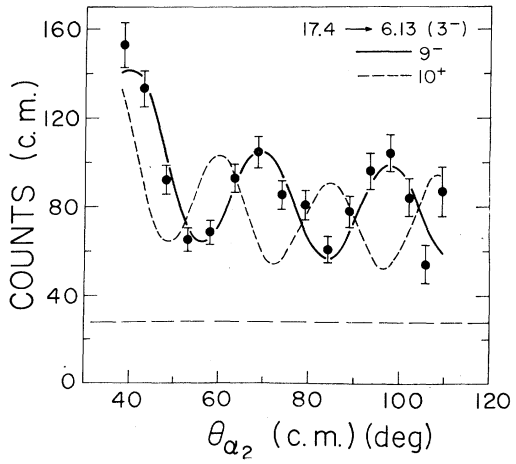

FIG. 13. Result of the triple correlation measurement for the 17.40-MeV state in ^{20}Ne. The curves are the best fits for the spins shown with the effect of hyperfine interaction included; the horizontal broken line indicates the value of the isotropic background extracted from the fit.

B. 17.40-MeV Level

The state at 17.40 MeV was known[14] to be very strongly excited in the ^{12}C$(^{12}$C, $\alpha)^{20}$Ne reaction at bombarding energies near 37 MeV, and the triple-correlation measurement was performed at a bombarding energy of 37.2 MeV. The triple correlation obtained for decays to the 6.13-MeV (3^-) state in ^{16}O is shown in Fig. 13: the errors shown are statistical. The values of the Q_k(HFI) obtained from the ^{16}O$(\alpha, \alpha'\gamma)^{16}$O measurement were used in the fits to the triple correlation of this state. The only assumption involved in the use of these values of the Q_k was that they did not change appreciably over the range of energies of the recoiling ^{16}O*(6.13-MeV) ions; however, as the ionic charge state fractions are predicted to be slowly changing functions of energy,[10] this assumption was expected to be a good one. The dashed horizontal line in Fig. 13 is the isotropic background extracted from the fit for $J^\pi = 9^-$; for the purposes of comparison the same background was used in obtaining the fit for $J^\pi = 10^+$. A plot of χ^2 versus

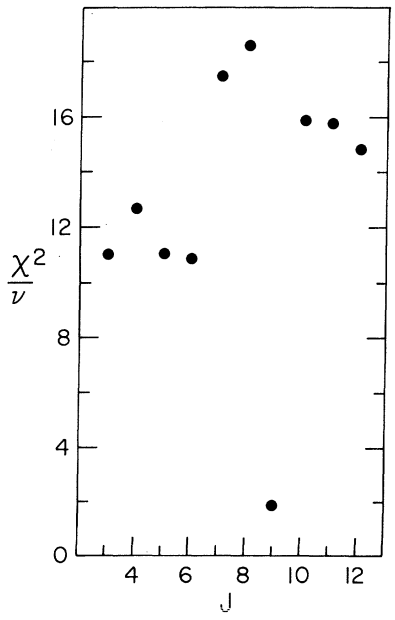

FIG. 14. Plot of normalized χ^2 of fits to the triple angular correlation of Fig. 13 for different values of the spin of the 17.40-MeV state in ^{20}Ne. The value of the isotropic background used in the fits was allowed to vary by 20% about the value obtained from the fit for spin and parity 9^-.

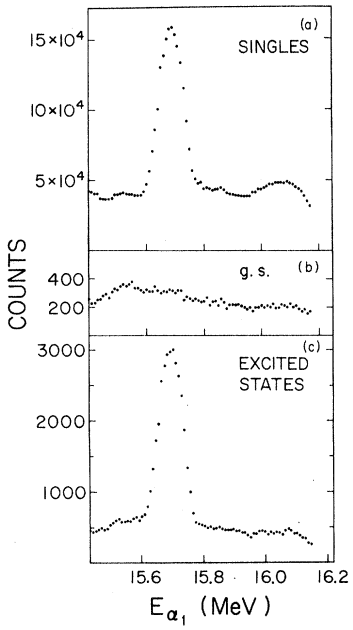

FIG. 15. Zero degree spectra in singles, in coincidence with decays to the ^{16}O ground state, and in coincidence with decays to excited states in ^{16}O. The strong peaks correspond to the 17.40-MeV state in ^{20}Ne.

J for the 17.40-MeV triple correlation is presented in Fig. 14; in obtaining the best fits for a given spin, the value of the isotropic background was allowed to vary by ±20% about the value obtained for $J^\pi = 9^-$. It is clear that an acceptable fit was obtained for $J^\pi = 9^-$ only. Hence, from the triple correlation of α-particle decays to the 6.13-MeV (3^-) state in ^{16}O, we have assigned $J^\pi = 9^-$ to the 17.40-MeV state in ^{20}Ne. Divided zero degree spectra, both in singles and in coincidence with decays to the ground state and to the unresolved first doublet (6.05-, 6.13-MeV) in ^{16}O are presented in Fig. 15. The spectra in Fig. 15 were obtained from a separate measurement. The peak-to-background ratio in Fig. 15(c) is consistent with the background obtained from the fit to the triple correlation of the 17.40-MeV state.

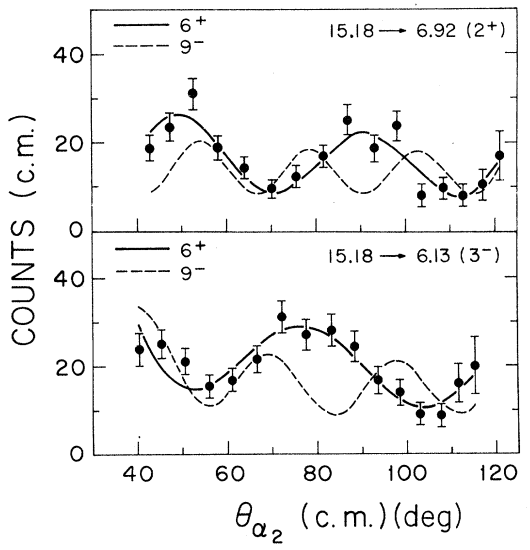

FIG. 16. Results of the triple correlation measurement on the 15.18-MeV state in ^{20}Ne. The curves are the best fits for the spins shown, and in the case of the correlation of decays to the 6.13-MeV (3^-) state in ^{16}O, the effect of hyperfine interaction has been taken into account.

C. 15.18-MeV Level

The state at 15.18 MeV in ^{20}Ne was studied by Panagiotou, Gove, and Harar[13] at a bombarding energy of 45 MeV. The maximum terminal voltage attainable with our accelerator restricted us to much lower ^{12}C energies, but a state at 15.18 ±0.02 MeV was known[15] to be strongly excited at bombarding energies around 36 MeV, and a triple-correlation measurement for this state was carried out at 36.3 MeV. The state was found to decay with almost equal strengths to the 6.13-MeV (3^-) and 6.92-MeV (2^+) states in ^{16}O, with only a very weak branch to the ^{16}O ground state.

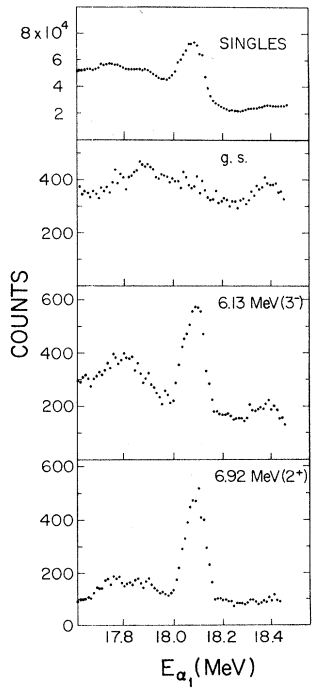

FIG. 17. Zero degree spectra in singles and in coincidence with decays to the ground state, the 6.05–6.13-MeV doublet, and the 6.92–7.12-MeV doublet in ^{16}O. The peak in three of the spectra corresponds to the 15.18-MeV state in ^{20}Ne.

The triple correlations for the decays to the 6.13- and 6.92-MeV levels in ^{16}O are shown in Fig. 16; the curves are the best fits for the spins shown. In the case of the correlation of α decays to the 6.13-MeV level, the Q_R(HFI) derived from the $^{16}O(\alpha, \alpha'\gamma)^{16}O$ correlation measurement were used, as the average recoil of the $^{16}O^*$(6.13-MeV) ions was again about 6 MeV. Both triple correlations yield an unambiguous spin and parity assignment of 6^+ to the 15.18-MeV level, and it can be seen that a 9^- assignment is in obvious disagreement with the data.

A separate measurement, in which only α_1-α_2 coincidences were stored and the energy signal from the zero degree detector was stored in place of E_γ, was performed at the same beam energy of 36.3 MeV for the purpose of determining the branching ratios of the decays of the 15.18-MeV state. Divided zero degree spectra from this run, in singles and in coincidence with α_2 decays to the ground state, first doublet (6.05-, 6.13-MeV) and second doublet (6.92-, 7.12-MeV) of ^{16}O, are presented in Fig. 17. The two members of these doublets were unresolved in the E_2 spectra due to the kinematic broadening of approximately 500 keV per slice. From the spectra of Fig. 17, the relative magnitudes of the branches of the 15.18-MeV state to the ground state, first doublet, and second doublet in ^{16}O were determined.

In order to obtain information on the branches to the individual members of the two doublets, a spectrum of γ rays (S_γ), in coincidence with α particles in the 15.18-MeV peak at zero degrees, was obtained from the α_1-γ coincidence events that were stored in the course of the triple-correlation measurement. Although the 6.92- and 7.12-MeV full-energy peaks were not resolved in this spectrum, a good estimate of the number of counts in the 7.12-MeV full-energy peak was obtained from a shape analysis of the high-energy portion of the strong 6.92-MeV full-energy peak. This estimate provided a limit on the magnitude of a possible branch of the 15.18-MeV level in ^{20}Ne to the 7.12-MeV level in ^{16}O. Only a limit was obtained since it was not possible to determine whether the decays to the 7.12-MeV level were from the 15.18-MeV level itself, or from broad low-spin states at the same excitation energy.

TABLE I. Branching ratios for the decays of the 15.18- and 17.40-MeV levels.

Final state in ^{16}O (MeV)	Branch (%) 15.18	17.40
g.s.	3 ± 3	<1
6.05	<6	<1
6.13	>43 } 49 ± 3	>99 } 100
6.92	>43	
7.12	<5 } 48 ± 3	<5

The 6.05-MeV (0^+) level in ^{16}O decays by internal pair production, and would contribute 511-keV γ rays to the γ-ray spectrum. However, the spectrum of a high energy γ ray alone also contains a 511-keV photopeak from pair production in the material surrounding the NaI(Tl) crystal, and the existence of a decay branch to the 6.05-MeV state could not be inferred simply from the presence of a 511-keV photopeak. This difficulty was resolved by measuring γ-ray spectra in coincidence with deuterons at zero degrees from the reaction ^{12}C-($^6Li, d\gamma)^{16}O$ with the NaI(Tl) crystals in the same geometry as in the triple-correlation measurements. At a ^6Li energy of 20 MeV, all four states of interest in ^{16}O (6.05, 6.13, 6.92, and 7.12 MeV) were strongly populated and were well resolved in the divided zero degree deuteron spectrum; separate γ-ray spectra were obtained from each of the four states in ^{16}O. The contributions of high-energy γ rays to the 511-keV photopeak in S_γ were estimated from the 6.13- and 6.92-MeV γ-ray spectra, and were subtracted. Any

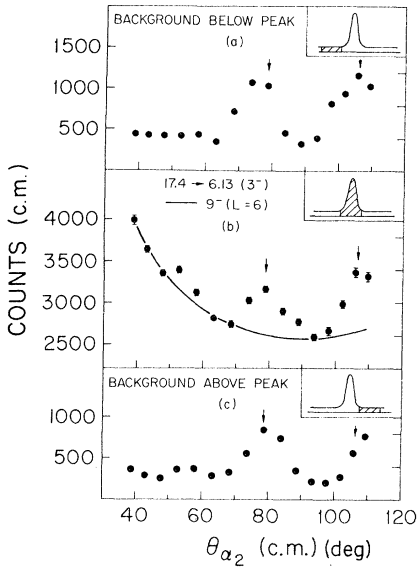

FIG. 18. Double (α_1-α_2) correlations of α_2 decays to the 6.13-MeV (3^-) state in ^{16}O from the regions of the zero degree spectrum (a) to the left of the 17.40-MeV peak, (b) the 17.40-MeV peak, and (c) to the right of the 17.40-MeV peak. The arrrows mark the positions of the background peaks in the correlation (b) due to Process II involving the 17.4-MeV and 15.9-MeV states in ^{20}Ne. The corresponding peaks in the correlations (a) and (c) are clearly displaced from the positions marked by the arrows.

excess of counts in the 511-keV photopeak was then attributed to decays of the 6.05-MeV level in ^{16}O. The number of excess counts, together with the γ-ray yield from the ^{12}C(^{6}Li, $d\gamma$) reaction populating the 6.05-MeV state, allowed a limit to be placed on the branch of the 15.18-MeV level in ^{20}Ne to the 6.05-MeV level in ^{16}O. Again, only a limit could be obtained by this method, as it was not possible to distinguish between decays from the 15.18-MeV level itself and decays from the broad states at the same excitation.

Similar procedures were followed to extract branching ratios for the decays of the 17.40-MeV state. The results for both states are given in Table I.

In addition to the triple correlations, α_1-α_2 double correlations were also obtained from the data with, on the average, 50 times as many counts per angle as the corresponding triple correlation. Figure 18(b) shows the α_1-α_2 correlation from the decay of the 17.40-MeV level in ^{20}Ne to the 6.13-MeV level in ^{16}O. The solid curve is the theoretical prediction [Eq. (1)] for $J^\pi = 9^-$, assuming that the α_2 decay proceeds by the lowest allowed L value ($L = 6$) only. The agreement between the prediction and the data is good except for the presence of peaks in the experimental correlation which are centered at $\theta_{\text{c.m.}} = 78$ and 107°. These peaks arise from the sequential process (Process II) ^{12}C(^{12}C, $\alpha_1^\dagger$)^{20}Ne*(X MeV)$\rightarrow$ ^{16}O*(6.13 MeV)+$\alpha_2^\dagger$, but with $\alpha_2^\dagger$ now detected at zero degrees, and $\alpha_1^\dagger$ detected in the slice detector. For a state at a given excitation energy, X, in ^{20}Ne, there is a unique angle (θ_x) at which an $\alpha_1^\dagger$ will have the same energy as an α_2 from the decay of the 17.40-MeV state in ^{20}Ne; conservation of energy and momentum then require that at zero degrees $\alpha_2^\dagger$ and α_1 also have the same energy. As we move away from θ_x, the energies at zero degrees of $\alpha_2^\dagger$ and α_1 separate, and the position of $\alpha_2^\dagger$ in the zero degree spectrum changes. Hence, a window on the 17.40-MeV peak in the zero degree spectrum selects a narrow energy range of $\alpha_2^\dagger$, and the $\alpha_1^\dagger$ in coincidence with these $\alpha_2^\dagger$ span a corresponding narrow angular range centered about θ_x. A state populated strongly in the reaction ^{12}C(^{12}C, $\alpha_1^\dagger$)^{20}Ne* (X MeV), with $\alpha_1^\dagger$ observed near θ_x, will then produce a peak in the α_1-α_2 correlation centered at θ_x. The choice of a different range of $\alpha_2^\dagger$ energies should change the angular position of the peak, and Figs. 18(a) and 18(c) show α_1-α_2 double correlations obtained from the regions of the zero degree spectrum to the left and to the right of the 17.40-MeV peak. The shifts in the positions of the peaks are evident, and the magnitudes of the shifts are in good agreement with calculations based upon the above identification of these peaks. The states in ^{20}Ne which produced the peaks were identified as the 17.40-MeV state itself ($\theta_x = 78°$) and the 15.9-MeV state ($\theta_x = 107°$).

Of course, the same mechanism operates to produce counts in the triple correlation at the same angles, but the effect on the triple correlation is small. The actual number of counts that Process II adds to the α_1-α_2 double correlation of the 17.40-MeV state at $\theta_x = 78°$ is less than 15% of the number of true α_1-α_2 double coincidences at that angle, and the relative magnitude of the effect must be similar in the triple correlation. As the angles at which Process II contributes to the triple correlation are known, and as the size of the effect is less than 2 standard deviations at these angles, it cannot affect the spin assignment derived from the triple correlation. Process II also contributes counts to the triple correlations from the 15.18-MeV state, but again the effect cannot change the 6^+ spin assignment derived from these correlations.

The earlier assignment[13] of 9^- to the 15.18-MeV level was made from the α_1-α_2 correlation of the weak ground-state branch. This 9^- assignment is in disagreement with the 6^+ assignment obtained in the present work, and this disagreement has been discussed in Ref. 6. A point not discussed in Ref. 6, however, is that the correlation of Ref. 13 exhibits a very pronounced peak at $\theta_{\text{lab}} = 71°$ which the authors incorrectly attribute to the correlation of a level in ^{20}Ne that was not resolved from the 15.18-MeV level in the zero degree spectrum. In fact, this peak is due to Process II involving the 15.9-MeV level in ^{20}Ne.

We have also studied the α decays of the level

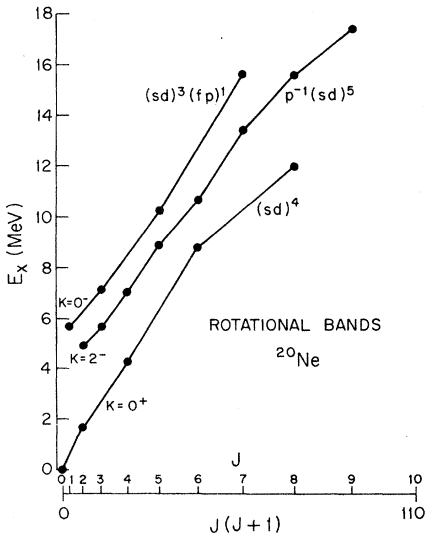

FIG. 19. Rotational band structure in ^{20}Ne.

at 13.33 MeV (7^-) using a similar experimental arrangement to that employed in the measurements of the branching ratios of the 15.18- and 17.40-MeV states. Two measurements were made with the slice detector centered at 45 and 90° to the beam direction, giving an α_1-α_2 angular correlation spanning 100° in the laboratory system. The branching ratios of the 13.33-MeV level were determined to be $43 \pm 1\%$ to the ^{16}O ground state and $57 \pm 1\%$ to the 6.13-MeV (3^-) state in ^{16}O. The α_1-α_2 correlation of decays to the ^{16}O ground state presented in Fig. 8 was obtained from this measurement.

VII. DISCUSSION

The rotational band structure of ^{20}Ne is shown in Fig. 19. In particular, the lowest negative-parity band is built on the 2^- level at 4.97 MeV. Prior to the present work, members of this band had been identified[3] as far as the 7^- level at 13.33 MeV, with an unnatural-parity state at 15.62 MeV[16] being a good candidate for the 8^- member. The available information[17] on the properties of this band is summarized in Table II, where the dimensionless reduced width of the ground-state decay of the 13.33-MeV state given in Ref. 17 has been corrected for the existence of the branch to the 6.13-MeV state. The reduced widths of the decays of the members of the band to the ^{16}O ground state are all small, consistent with the predominant shell-model configuration[18] of the intrinsic state being $(1p)^{-1}(2s\text{-}1d)$,[5] which has very little overlap with an α particle plus the ^{16}O ground state. As decays to the ^{16}O ground state must take place via small components of the wave functions, the variation in the ground-state widths among the members of the band is not unexpected. Furthermore, the intrinsic state of this band should have a large overlap with an α particle plus the 6.13-MeV (3^-) level in ^{16}O which is built[18] out of $(1p)^{-1}(2s\text{-}1d)^1$ excitations, and this is reflected in the appreciable reduced width of the decay of the 13.33-MeV level to the 6.13-MeV state in ^{16}O.

The energy of the 17.40-MeV (9^-) state in ^{20}Ne is such that it fits very nicely into the lowest negative-parity band. If one assumes similar reduced widths for the decays of the 13.33- and 17.40-MeV levels to the 6.13-MeV state in ^{16}O, then the 1% limit on the ground-state branch of the 17.40-MeV level implies a ground state reduced width of less than 2×10^{-3}. This very small reduced width, together with the position of the state on an energy versus $J(J+1)$ plot, provides strong evidence for the identification of the 17.40-MeV level in ^{20}Ne as the 9^- member of the lowest negative-parity band. All other known[19] 9^- states in ^{20}Ne have considerable reduced widths for the decay to the ground state of ^{16}O, and are therefore not likely candidates for a member of this band.

Plots of moment of inertia versus ω^2 (as defined by Johnson, Ryde, and Sztarkier[20]) are presented in Fig. 20 for the $K^\pi = 0^+$ and $K^\pi = 2^-$ bands in ^{20}Ne. These plots emphasize the similarity of the "backbending" that occurs in both bands between spins 6 and 8.

Prior to the present work, a state in ^{20}Ne at 15.18 MeV that was strongly excited in the ^{12}C-(^{12}C, α)^{20}Ne reaction, had been assigned spin and parity 9^- by Panagiotou, Gove, and Harar,[13] an assignment which would seem to have important implications concerning the band structure of ^{20}Ne. In particular, one would expect the lowest 9^- state in ^{20}Ne to be the 9^- member of the lowest negative-parity band which we have identified as the 17.40-MeV state. The presence of a 9^- level at 15.18 MeV was therefore rather surprising, and led Vogt[21] to propose the existence of a "superband"

TABLE II. α-decay widths in the $K^\pi = 2^-$ band of ^{20}Ne.

E_{exc} (MeV)	J^π_i	J^π_f	L	Γ_0 (keV) [a]	Γ_{exp} (keV)	$\theta^2\times10^3$ [b]
5.618	3^-	0^+	3	54×10^{-6}	$(3.1\pm0.7)\times10^{-6}$ [c]	57 ± 13
8.447	5^-	0^+	5	5.4	<0.2 [d]	<37
13.333	7^-	0^+	7	94	0.19 ± 0.07 [e]	2.0 ± 0.7
		3^-	4	1.1	0.25 ± 0.09	220 ± 80

[a] $\Gamma_0 = 2kR/(F_L^2 + G_L^2)\,\hbar^2/\mu R^2$ evaluated for $R = 5.134$ fm (following Ref. 17).

[b] $\theta^2 = \Gamma_{exp}/\Gamma_0$.

[c] O. Häusser, T. K. Alexander, A. B. McDonald, G. T. Ewan, and A. E. Litherland, Nucl. Phys. A168, 17 (1971).

[e] Reference 17; corrected for the 57% branch to the 3^- level.

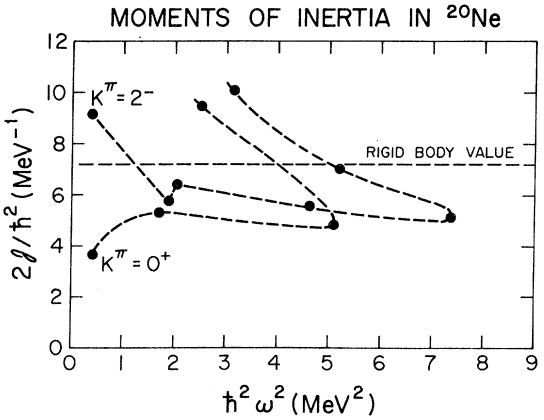

FIG. 20. Moments of inertia versus ω^2 for the $K^\pi = 0^+$ and $K^\pi = 2^-$ bands in ^{20}Ne. The rigid body value of the moment of inertia was calculated for a radius of $1.3A^{1/3}$ fm and for a deformation determined from the known quadrupole moment of the 1.63-MeV (2^+) state.

with a very large moment of inertia, of which both the 13.33-MeV (7^-) and 15.18-MeV levels were members. We have assigned spin and parity 6^+ to a level at 15.18 ± 0.02 MeV, observed in the same reaction although at a lower beam energy than that used in the earlier measurement. As discussed in Ref. 6, this new assignment would seem to cast some doubt upon the existence of a low-lying negative-parity superband in ^{20}Ne, and repeating the experimental work of Ref. 13 would help to resolve any remaining doubt.

In conclusion, a new method has been developed for assigning spins to natural-parity states that are strongly populated in reactions of the type ^{12}C(^{12}C, α)^{20}Ne, but which α decay to states of nonzero spin. The method has been applied to the determination of the spins and parities of states in ^{20}Ne at 17.40 MeV (9^-) and 15.18 MeV (6^+). The 17.40-MeV state has been identified as the 9^- member of the lowest negative-parity band. These spin assignments are consistent with the prediction that reactions of the above type should selectively populate high-spin states.

APPENDIX

Derivation of the Triple Correlation Formula

We wish to derive an expression for the α_1-α_2-γ correlation from reactions of the type

$$^{12}\mathrm{C} + {}^{12}\mathrm{C} \rightarrow {}^{20}\mathrm{Ne}^*(J_A M_A) + \alpha_1 \hookrightarrow {}^{16}\mathrm{O}^*(J_F M_F) + \alpha_2(L\Lambda) \hookrightarrow {}^{16}\mathrm{O}(J_F M_F) + \gamma(L_\gamma \Lambda_\gamma).$$

The quantization axis is chosen to lie along the beam direction. The first emitted α particle is detected at 0°, and therefore only the $M_A = 0$ substate in ^{20}Ne* can be populated. It follows that the density matrix of the ensemble of ^{20}Ne* nuclei is simply

$$\rho_{M_A M'_A} = \delta_{M_A 0}\delta_{M'_A 0}$$

and the density matrix of the ^{16}O* + α_2 system is then

$$\rho^{(^{16}\mathrm{O}^*)}_{M_B M'_B}\, \rho^{(\alpha_2)}_{L,-M_B;L',-M'_B} = (J_B M_B L - M_B | J_A 0)(J_B M'_B L' - M'_B | J_A 0) \langle \| L \| \rangle \langle \| L' \| \rangle^*. \tag{1}$$

The reduced matrix elements $\langle \| L \| \rangle$ are defined in Sec. II.

The ensemble of ^{16}O* nuclei with density matrix $\rho_{M_B M'_B}$ then breaks up into ^{16}O + γ with density matrix elements $\rho^{(^{16}\mathrm{O})}_{M_F M'_F}\, \rho^{(\gamma)}_{\Lambda_\gamma \Lambda'_\gamma}$, where we have assumed that the γ ray has pure multipolarity.

Formally, the angular correlation may be written[22]

$$W = \mathrm{Tr}(\rho\epsilon),$$

where ρ is the density matrix of the final state, and ϵ is the efficiency matrix which describes the position and sensitivity of the detectors. In the present case

$$W = \sum_{\substack{M_B M'_B \\ L L'}} \rho^{(\alpha_2)}_{L,-M_B;L',-M'_B}\, \epsilon^{(\alpha_2)}_{L',-M'_B,L,-M_B} \left\{ \sum_{\substack{M_F M'_F \\ \Lambda_\gamma \Lambda'_\gamma}} [\rho^{(^{16}\mathrm{O})}_{M_F M'_F}\, \rho^{(\gamma)}_{\Lambda_\gamma \Lambda'_\gamma}]\, \delta_{M_B, M_F + \Lambda_\gamma}\, \delta_{M'_B, M'_F + \Lambda'_\gamma}\, \epsilon^{(^{16}\mathrm{O})}_{M'_F M_F}\, \epsilon^{(\gamma)}_{\Lambda_\gamma \Lambda'_\gamma} \right\}. \tag{2}$$

However, the expression $\{\ \}$ is simply the angular distribution of γ rays from a system for which only the $(M_B M'_B)$ element of the density matrix is nonzero, and may be written

$$W_{M_B M'_B}(\Omega) = \sum_{k q} (-)^{J_B - M'_B}\, \rho^{(^{16}\mathrm{O}^*)}_{M_B M'_B}\, (J_B M_B J_B - M'_B | kq) R_k(L_\gamma L_\gamma J_B J_F) \left(\frac{4\pi}{2k+1}\right)^{1/2} Q_k\, Y^q_k(\Omega_\gamma), \tag{3}$$

where the R_k are the angular distribution coefficients of Rose and Brink,[7] and the Q_k take the finite detector size into account for cylindrical γ-ray detectors. The efficiency matrix for a point particle detector at (θ, φ) is simply

$$\epsilon_{LM,L'M'} = Y^M_L{}^*(\theta, \varphi) Y^{M'}_{L'}(\theta, \varphi). \tag{4}$$

Substituting (3) and (4) into (2), and using (1), we arrive at an expression for the α_1-α_2-γ correlation, where α_1 is detected at 0°, α_2 is detected at $(\theta_{\alpha_2}, 0)$, and γ is detected at (θ_γ, φ), φ being the relative azimuthal angle of the particle and γ-ray detectors:

$$W(\theta_{\alpha_1} = 0°; \theta_{\alpha_2}, \theta_\gamma, \varphi) = \sum_{\substack{M_B M'_B \\ L L'}} (J_B M_B L - M_B | J_A 0)(J_B M'_B L' - M'_B | J_A 0) \langle \| L \| \rangle \langle \| L' \| \rangle^* Y^{-M_B}_L(\theta_{\alpha_2}, 0) \times Y^{-M'_B}_{L'}{}^*(\theta_{\alpha_2}, 0) \sum_{k q} (-1)^{J_B - M'_B} \left(\frac{4\pi}{2k+1}\right)^{1/2} R_k(L_\gamma L_\gamma J_B J_F) Q_k (J_B M_B J_B - M'_B | kq) Y^q_k(\theta_\gamma, \varphi).$$

†Work supported by the National Science Foundation.

[1]A. E. Litherland, J. A. Kuehner, H. E. Gove, M. A. Clark, and E. Almqvist, Phys. Rev. Lett. 7, 98 (1961).
[2]J. A. Kuehner and J. D. Pearson, Can. J. Phys. 42, 477 (1964).
[3]J. A. Kuehner and E. Almqvist, Can. J. Phys. 45, 1605 (1967).
[4]P. J. M. Smulders, C. Broude, and A. E. Litherland, Can. J. Phys. 45, 2133 (1967).
[5]J. A. Kuehner and R. W. Ollerhead, Phys. Lett. 20, 301 (1966).
[6]R. W. Zurmühle, D. P. Balamuth, L. K. Fifield, and J. W. Noé, Phys. Lett. 44B, 453 (1973).
[7]H. J. Rose and D. M. Brink, Rev. Mod. Phys. 39, 306 (1967).
[8]N. J. Hansen, D. J. Henderson, and R. G. Scott, Nucl. Instrum. Methods 105, 293 (1972).
[9]T. K. Alexander and K. W. Allen, Can. J. Phys. 43, 1563 (1965).
[10]J. B. Marion and F. C. Young, *Nuclear Reaction Analysis, Graphs and Tables* (North-Holland, Amsterdam, 1968), p. 43.
[11]Z. Berant, M. B. Goldberg, G. Goldring, S. S. Hanna, H. M. Loebenstein, I. Plesser, M. Popp, J. S. Sokolowski, P. N. Tandon, and Y. Wolfson, Nucl. Phys. A178, 155 (1971), and references therein.
[12]R. W. Zurmühle, P. F. Hinrichsen, C. M. Fou, C. R. Gould, and G. P. Anastassiou, Nucl. Instrum. Methods 71, 311 (1969).
[13]A. D. Panagiotou, H. E. Gove, and S. Harar, Phys. Rev. C 5, 1995 (1972).
[14]R. Middleton, H. T. Fortune, and R. R. Betts, private communication. The energy of the state is 17.40 ± 0.02 MeV.
[15]R. Middleton, H. T. Fortune, and R. R. Betts, private communication.
[16]A. D. Panagiotou, Phys. Lett. 31B, 361 (1970).
[17]O. Häusser, A. J. Ferguson, A. B. McDonald, I. M. Szöghy, T. K. Alexander, and D. L. Disdier, Nucl. Phys. A179, 465 (1972).
[18]M. Harvey, in *Advances in Nuclear Physics*, edited by M. Baranger and E. Vogt (Plenum, New York, 1968), Vol. 1.
[19]C. Bergman and R. K. Hobbie, Phys. Rev. C 3, 1729 (1971).
[20]A. Johnson, H. Ryde, and J. Sztarkier, Phys. Lett. 34B, 605 (1971).
[21]E. Vogt, Phys. Lett. 40B, 345 (1972).
[22]A. J. Ferguson, *Angular Correlation Methods in Gamma-ray Spectroscopy* (North-Holland, Amsterdam, 1965).